Surface Characterization and Protein Interactions of Segmented Polyisobutylene-Based Thermoplastic Polyurethanes

David Cozzens, Arnold Luk, Umaprasana Ojha, Marina Ruths, and Rudolf Faust[*]

Department of Chemistry, University of Massachusetts Lowell

One University Avenue, Lowell, MA 01854

SUPPORTING INFORMATION

Contact area in colloidal probe measurements

The radius *a* of the contact area between the protein-covered colloidal probe and the polymer substrates was estimated using the Thin-Coating Contact Mechanics (TCCM) model for adhesive contact developed by Reedy.[1,2] In this model, the probe (sphere) and the flat substrate are assumed to be rigid, which is a reasonable assumption at low loads in our experiment, where the deformations occur mainly in the compliant protein layer. In the model, the substrate is assumed to be perfectly flat, whereas our polymer has some roughness preventing the protein film from making contact over parts of the projected contact area. This is also reflected in the pull-off forces (Figure 5) which are lower than those expected for a perfectly flat substrate. To obtain an estimate of the radius of the contact area, we therefore used the experimental values of the work of adhesion ($W = F/(2\pi R)$ with F/R from Figure 5), the radius of curvature of the probe (R = 5 μm), and the thickness of the protein layer (h, from Figure 2b). The Poisson ratio of the protein layers was assumed to be 0.4, and for the Young's modulus of the protein layers we used a value of 1.55 MPa reported for Fg.[3] The radii of the contact areas were calculated as a function of normal force at the two limits of the TCCM model (the DMT-like limit for low adhesion and stiff coatings

and the JKR-limit for large adhesion and soft coatings), as shown in Figure S1. At normal forces corresponding to the ones used in the force measurements (Figure 5), the radii were a = 100–250 nm (and the diameter of the contact area thus 200–500 nm) during compression and a = 100–175 nm at the point of separation (spontaneous jump apart). Thus we conclude that compared to the domain sizes in Figure 1, the adhesion forces measured were those between the protein monolayer and a good representation of the different chemical groups present on the polymer surfaces.

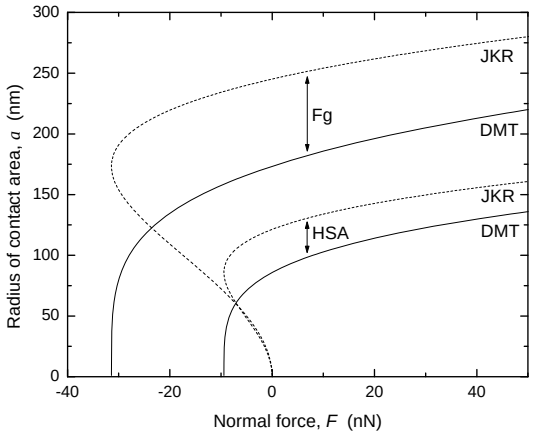

Figure S1. Radius of the contact area during force measurements with the colloidal probe, as estimated from the TCCM model with R = 5 μm, h_{Fg} = 15 nm, h_{HSA} = 3 nm, W_{Fg} = 1 mJ/m^2, and W_{HSA} = 0.3 mJ/m^2.

Preparation of colloidal probes

The colloidal probe consisted of a gold sphere (radius 2.4-8.8 μm) attached to a tipless cantilever (Mikromasch, NSC12/tipless/AlBS). The probe has a contact area large enough to provide an average over the phase-separated domains of the TPU surfaces as estimated above. The resonant frequency, resonant amplitude, and Q value of the cantilevers were determined before the spheres were attached so

that the spring constant could be determined. Typical probes had resonant frequencies of ~20-21 kHz, and spring constants 0.30 – 0.35 N/m. The probes were prepared by using the AFM stage as a micromanipulator to pick up a minute amount of glue with the end of the cantilever and then a gold sphere. After curing of the glue, the colloidal probes were imaged to determine their smoothness, uniformity, and radius.[4] This was done by scanning the colloidal probe over a calibration sample (Mikromasch, TGT01) with a regular array of sharp tips with radii of < 10 nm, i.e., much less than the colloidal probe. The resulting AFM image is a "reverse image" of the colloidal probe from which its radius of curvature can be extracted by fitting the equation for a sphere to the top portion of the data. A representative cross-sectional analysis from such an image is shown in Figure S2.

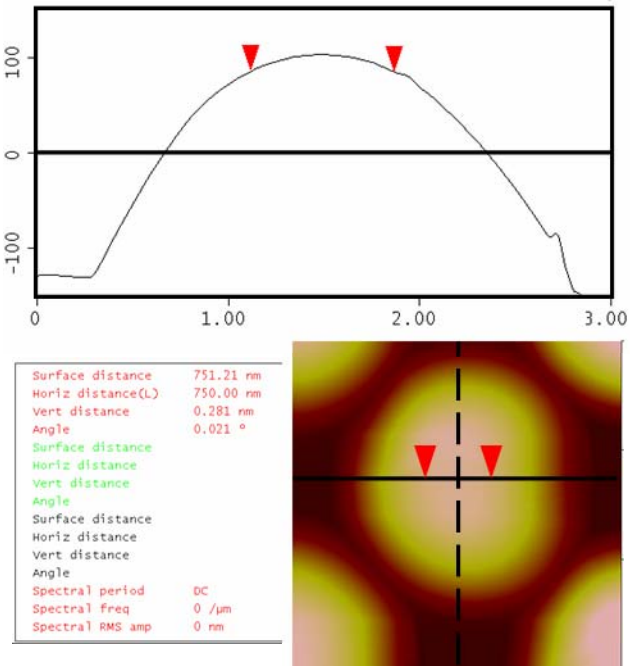

Figure S2. Cross-sectional analysis of colloidal probe.

Force measurements with bare gold probe

Figure S3 shows a representative force curve for a bare gold sphere interacting with a P55D surface in PBS. The curve shows a sharp and clear pull-off at very low separation. This curve is of a very

different nature than those generated with protein-coated colloidal probes as shown in Figure 4, which depict the gradual unraveling of protein chains.

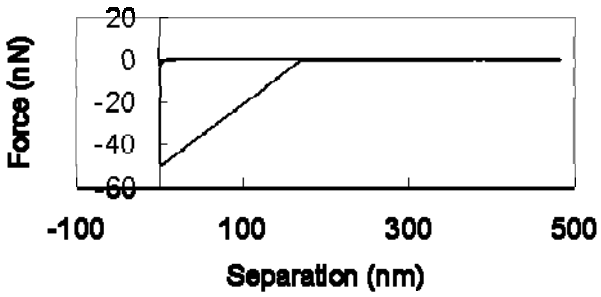

Figure S3. Interaction forces between SIBS and a bare Au probe (R = 4.1 μm) in PBS buffer.

Negative control showing selective GPIIb-IIIa binding to Fg

Figure S4 shows the raw QCM-D data from a trial consisting of adsorption of a BSA monolayer, followed by the BSA blocking step, followed by GPIIb-IIIa binding.[5] The absence of net shifts in frequency or dissipation between time points e and f indicate that there was no binding of GPIIb-IIIa to the BSA monolayer.

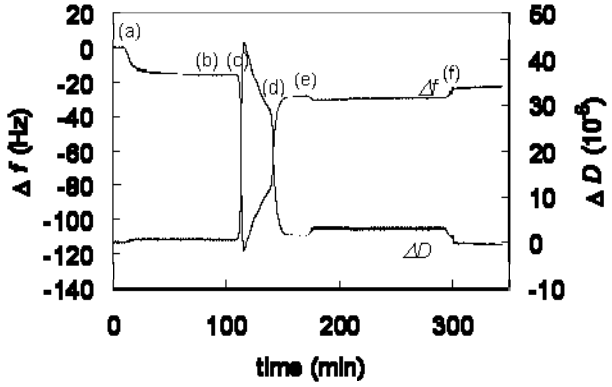

Figure S4. Negative control showing selective GP binding to Fg. (a) BSA solution (833 μg/mL), (b) Tris rinse, (c) BSA blocking (10 wt.%), (d) Tris rinse, (e) GP IIb-IIIa, (f) Tris rinse.

Correlation of GP/Fg binding ratio to the % Fg adsorbed.

Figure S5 shows the spread of data and the corresponding trend line for the ratio of GPIIb-IIIa to Fg at different Fg coverage.[5] The value for 100% coverage is taken from experiments analogous to those performed to generate Table 4. These data points are from 4 different surfaces: P80A, SIBS, poly(vinylidene fluoride-*co*-hexafluoropropylene), and poly(D,L-lactide-*co*-glycolide), and all show the same trend. This data indicates that there is steric crowding at higher percent coverage of the surface which limits GPIIb-IIIa binding to Fg.

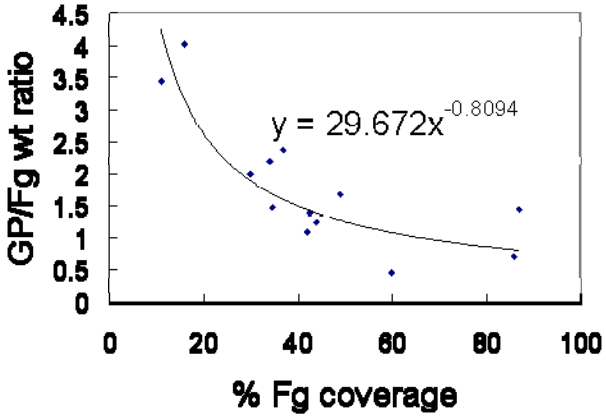

Figure S5. Correlation of GP/Fg to %Fg adsorbed.

References

[1] Reedy, E.D. Jr. *J. Mater Res.* **2006,** *21,* 2660-2668.

[2] Reedy, E.D. Jr. *J. Mater. Res.* **2007,** *22,* 2617-2622.

[3] Koo, J.; Rafailovich, M.H.; Medved, L.; Tsurupa, G.; Kudryk, B.J.; Liu, Y.; Galanakis, D.K. *J. Thromb. Haemost*. **2010**, *8*, 2727-2735.

[4] Neto, C.; Craig, V.S.J. *Langmuir* **2001,** *17,* 2097-2099.

[5] Luk, A.; Cozzens, D.; Faust, R. To be submitted.